J Mater Sci (2009) 44:6286–6293
DOI 10.1007/s10853-009-3865-1

Fumed silica/polymer hybrid nanoparticles prepared by redox-initiated graft polymerization in emulsions

Mao Peng · Zhangjie Liao · Zhongming Zhu · Honglei Guo · Huijun Wang

Received: 30 May 2009 / Accepted: 31 August 2009 / Published online: 11 September 2009

Abstract Hybrid particles comprising aggregated fumed silica nanoparticles as the core and hydrophobic polymers existing around the nanoparticles were prepared by 'grafting from' polymerization in emulsions. The emulsion polymerization employed cetyltrimethylammonium bromide (CTAB) as a cationic surfactant and sodium dodecyl sulfate (SDS) as an anionic surfactant, respectively, to stabilize the emulsion polymerization. The polymerization was initiated by the redox reaction between ceric ion Ce(IV) and the amine groups on the surfaces of aminated fumed silica nanoparticles that were modified by 3-aminopropyltriethoxysilane. Infrared spectroscopy and thermogravimetric analysis demonstrated that both poly(methyl methacrylate) (PMMA) and polystyrene (PS) were successfully grafted onto the fumed silica surface. The type of surfactant greatly affected the grafting ratio, monomer-to-polymer conversion, and morphology of the product. When CTAB was used as the surfactant, both the grafting ratio and monomer-to-polymer conversion were lower than when SDS was used, but transmission electron microscopy and light scattering analysis indicated that most of the resultant particles were sub-100 nm hybrid nanoparticles with a non-spherical shape and particles sizes of 75–90 and 57–85 nm for PMMA and PS-grafted fumed silica, respectively. Whereas, when SDS was used as the surfactant, the particles agglomerated to form large irregular clusters or even networks, possibly due to the electrostatic attractions between SDS and Ce(IV) and/or the aminated fumed silica nanoparticles in aqueous solution.

M. Peng (✉) · Z. Liao · Z. Zhu · H. Guo · H. Wang
Department of Polymer Science and Engineering, Zhejiang University and Key Laboratory of Macromolecular Synthesis and Functionalization, Ministry of Education, Hangzhou 310027, China
e-mail: pengmao@zju.edu.cn

Introduction

The preparation of hybrid materials consisting of organic polymers with incorporated inorganic or metallic nanoparticles, such as silica, titanic dioxide, iron oxide magnetic nanoparticles, gold, and semiconductor nanoparticles (quantum dots) etc., has been an area of increasing research activity [1–7]. The hybrid materials can be either isolated nanoparticles with a well-defined core–shell structure [1, 2] or nanoaggregates with a number of inorganic or metallic nanoparticles embedded in polymer matrices [3–6]. These hybrid materials are potentially applied in diverse fields such as catalysis, nanosensors, bioseparation, and bioimaging, etc. At the same time, hybrid polymer/inorganic materials often have improved mechanical and thermal properties, compared with neat polymers [1–8].

To prepare hybrid materials, a number of 'grafting onto' or 'grafting from' approaches have been developed to graft polymers onto the surface of inorganic nanoparticles. The former involves reacting end-functionalized polymers directly with the particles modified with suitable functional groups [9–11] or employs nanoparticles grafted with methacryloxy(propyl)trimethoxysilane as seeds for polymerizations in emulsions [12, 13], miniemulsions [14] or microemulsions [15]. The silica nanoparticles are decorated with methacrylic double bonds and take part in the polymerization, so as to be covalently bonded to the polymer shells. Alternatively, the 'grafting from' approach involves immobilizing initiators on the surface of the particles followed by in situ surface-initiated polymerization to generate tethered polymers brushes [16–18]. Because the

polymer chains are covalently bonded to the inorganic surfaces, the polymer brushes are robust and resistant to common chemical environmental conditions. Furthermore, the combination of the 'grafting from' approaches with controlled/living free radical polymerizations such as atom transfer radical polymerization (ATRP) [1, 3, 19–21], reverse ATRP [22], reversible addition–fragmentation chain transfer [23, 24], and nitroxide-mediated processes [25–29], allows manipulating the molecular weight and polydispersity of the grafted polymer brushes.

On the other hand, many previous studies have demonstrated that the redox reaction between ceric ion Ce(IV) and reducing agents, such as polymers containing alcoholic hydroxyl, amine, mercapto or amide groups, can initiate the graft polymerization of unsaturated monomers onto the reducing agents [30–34]. Ce(IV) ions can form active sites onto the reducing agents by a single electron-transfer process [35, 36], which prevents the formation of homopolymer and results in high grafting ratios and monomer-to-polymer conversions. Preparation of polymer brushes on aminated glass substrates by Ce(IV)-initiated graft polymerization has been documented [37], therefore, it is reasonable to expect that polymer encapsulated inorganic nanoparticles can be obtained by redox-initiated graft polymerization. In our previous study [38], we reported on the preparation of polymer encapsulated silica nanoparticles (prepared using the Stöber method) by the Ce(IV)-initiated polymerization. It was found that, when hydrophilic polymers were grafted to the silica nanoparticles, the polymerization process was rather stable and well-defined nanoparticles with a core–shell structure could be obtained. But for hydrophobic polymers, macroscopic agglomeration formed and a large amount of precipitation appeared during polymerization. It was impossible to obtain polymer encapsulated particles with particle sizes below 100 nm.

In this study, we investigated the redox-initiated graft polymerization of hydrophobic monomers, such as methyl methacrylate (MMA) and styrene, on aminated fumed silica nanoparticles in the presence of surfactants, which successfully prevented macroscopic agglomeration and the formation of precipitation throughout the graft polymerization process. Ceric ammonium nitrate (CAN) was used as the oxidant and the aminated fumed silica nanoparticles worked as both the reductant and the substrate for the graft polymerization. Commercially available fumed silica can facilitate the scale up of the present process to an industrial level in the future. Cationic cetyltrimethylammonium bromide (CTAB) and anionic sodium dodecyl sulfate (SDS) were used as the surfactants for comparison. It was found that both the type of monomer and surfactant significantly influenced the grafting ratio, monomer-to-polymerization conversion and the size and morphology of the resultant products.

Materials and methods

Materials

Commercial available fumed silica (AEROSIL 200, Degussa, Germany) has a surface area to volume ratio of 200 ± 25 m^2/g. The monomers MMA and styrene were purified by washing with an aqueous solution of sodium hydroxide (5 wt%) three times and deionized water repeatedly, until the pH value of the washing water was reduced to 7, dried over anhydrous magnesium sulfate overnight, then distilled over calcium hydride under vacuum. The distillates were stored at -4 °C before use. Ethanol, methanol, nitric acid, CAN, anhydrous magnesium sulfate, 3-aminopropyltriethoxysilane (APTES), CTAB, and SDS were of analytical grades and were used as received.

Modification of fumed silica nanoparticles with APTES

Amination of the fumed silica nanoparticles was achieved by reacting silica with APTES in ethanol followed by agitating under fierce stirring for 48 h at 50 °C. The weight ratio between APTES and silica was 2:1. To remove unreacted APTES, the suspension of the fumed silica nanoparticles was centrifuged at 10000 rpm for 30 min. After the supernatant was decanted, the precipitates were collected and redispersed in ethanol by sonication. Centrifugation and redispersion were repeated three times. To remove the large silica agglomerates formed during the amination reaction, the purified product was redispersed in a diluted aqueous solution of nitric acid (0.14 mol/L) by magnetic stirring for 15 min and sonication for 30 min, and allowed to stand overnight at room temperature, then the upper layer of the stable suspension was carefully collected. A small amount of the suspension was dried to determine the solid content of the suspension. Finally, the solid content of the suspension was diluted to 1 mg/mL by adding the aqueous solution of nitric acid (0.14 mol/L).

Preparation of fumed silica/polymer hybrid particles

The polymer-grafted fumed silica particles were referred to as fumed silica/PS and fumed silica/PMMA hybrid particles, respectively. For the fumed silica/PMMA hybrid particles, 200 mL of the abovementioned suspension of aminated fumed silica was purged by nitrogen for 30 min and 1.07 g of CTAB or 0.87 g SDS and 2 mL of purified MMA were added and magnetically stirred for 10 min and then sonicated for 30 min. After the suspension was heated to 40 °C, 0.14 g of CAN was rapidly added to the suspension under the protection of nitrogen to initiate the polymerization. The polymerization was allowed to proceed under 40 °C for 12 h. The yellowish emulsion faded

Table 1 Recipes for the preparation of silica/polymer hybrid nanoparticles

Sample	Styrene	MMA	Aminated fumed silica (g)	CAN (g)	Aqueous solution of nitric acid (0.14 mol/L) (mL)	CTAB	SDS
1	1.6 mL	/	0.2	0.14	200	1.07 g	/
2	/	2 mL	0.2	0.14	200	1.07 g	/
3	1.6 mL	/	0.2	0.14	200	/	0.87 g
4	/	2 mL	0.2	0.14	200	/	0.87 g

gradually, indicating the occurrence of reduction of Ce(IV) to Ce(III). After polymerization, the product was precipitated from the emulsion by adding anhydrous magnesium sulfate, separated by filtration and purified by washing with water and methanol for three times, respectively. The product, fumed silica/PMMA hybrid nanoparticles, in a form of white powder was obtained after drying under vacuum at 50 °C. Fumed silica/PS hybrid nanoparticles were prepared in a similar way, in which the amount of styrene was 1.6 mL. The recipe of the emulsion polymerization is summarized in Table 1.

Characterizations

To observe the morphology, the pristine fumed silica nanoparticles were dispersed in methanol and dipped onto copper grids covered with formvar film, dried and observed by transmission electron microscopy (TEM, M-200CX, JEOL, Japan) at a voltage of 120 kV. For the aminated fumed silica, the particles were dispersed in a diluted aqueous solution of nitric acid. For the hybrid nanoparticles, the as-prepared aqueous suspension of the hybrid nanoparticles was diluted to a solid content of about 0.05 wt% and dipped onto a copper grid for the TEM observation. The particle sizes were analyzed by dynamic light scattering on a Brookhaven BI-90 plus Particle Size Analyzer (Brookhaven Instruments Corp., USA). FTIR spectra were recorded by using KBr pellets on a Bruker Vector 22 spectrometer (Germany). Thermogravimetric measurements were performed on a Perkin-Elmer Pyris 1 TGA (USA) at a heating rate of 20 °C/min from 120 to 900 °C in nitrogen atmosphere. According to the TGA result, the grafting ratio, defined as the weight of polymers grafted on 100 g of silica, is given by the following formula:

$$W_g = \Delta m/(m - \Delta m) \times 100 \quad (1)$$

where W_g is the grafting ratio, m is the weight of the initial sample, and Δm is the weight loss after pyrolysis.

The conversion of graft polymerization, namely the monomer-to-polymer conversion, which is defined as the ratio between the amount of grafted polymers and the amount of monomer used, can be calculated by the following formula:

$$\text{Conversion} = W_g/W_m \times 100 \quad (2)$$

where, W_m is the weight of monomer used for 100 g silica in the graft polymerization.

Results and discussion

Mechanism of the graft polymerization

According to the literature [39, 40], the mechanism of the graft polymerization initiated by a redox pair of ceric ion/amine is depicted in Fig. 1. The redox reaction between Ce(IV) and amine groups immobilized on the surface of silica nanoparticles leads to the formation of intermediate radicals, in which the free radical locates at the position of the α-carbon atom. Then, the free radical is transferred to the vinyl monomer and initiates polymerization. According to this mechanism, the graft polymerization starts from the surface of the aminated silica nanoparticles. This mechanism was experimentally supported by a control experiment, in which bare nanoparticles of fumed silica were employed to replace the aminated fumed silica nanoparticles and all other experimental conditions were the same, but neither graft polymerization nor homopolymerization was observable.

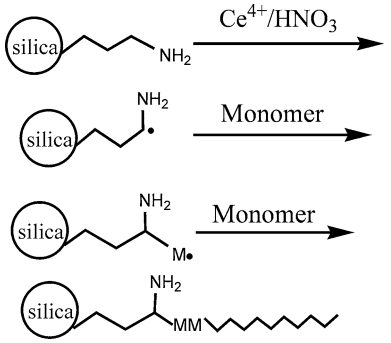

Fig. 1 The mechanism of the redox-initiated graft polymerization on aminated silica nanoparticles

IR spectra

Figure 2 presents the IR spectra of the pristine fumed silica, aminated fumed silica, fumed silica/PMMA, and fumed silica/PS hybrid particles prepared in emulsions using CTAB and SDS as surfactants, respectively. For all the samples, the strong absorption band at about 1097 cm^{-1} is assigned to the stretching vibration of Si–O–Si in the fumed silica. In the spectrum of aminated fumed silica (Fig. 2b), the characteristic vibration band of amino group appears at around 3297 cm^{-1}, indicating that APTES is successfully immobilized on the surface of fumed silica nanoparticles. For all the polymer encapsulated fumed silica prepared from emulsions with either CTAB or SDS as the surfactants, the adsorption bands of the polymers can be easily observed. For example, in the spectra of fumed silica/PS hybrid nanoparticles (Fig. 2c, e), the adsorption bands at 3020, 1601, 1490, 760, and 700 cm^{-1} can be ascribed to the stretching of C–H on the aromatic rings of PS. The adsorption bands at 2000–1660 cm^{-1} are ascribed to the vibration of carbon–carbon double bonds in the aromatic rings of PS and the bands at 2920 and 2850 cm^{-1} are ascribed to the C–H stretching vibration of the methylene groups (–CH_2–) in the macromolecular chains of PS. As to the PMMA-grafted fumed silica (Fig. 2d, f), a strong absorption band appeared at about 1735 cm^{-1} due to the stretching vibration of the ester carbonyl group (>C=O) of PMMA. At the same time, two obvious peaks appear at 1380 and 1465 cm^{-1} due to the bending vibration of methyl group (–CH_3) in PMMA. Therefore, the IR spectra indicate that for both CTAB and SDS as the surfactant, the two polymers PMMA and PS have been successfully grafted onto the surface of the fumed silica nanoparticles. At the same time, the IR spectra also indicate that the grafting ratios of the two polymers are larger when SDS was used as the surfactant, because the relative intensity of the characteristic bands of the polymers (Fig. 2e, f) is much higher than those when CTAB was used as the surfactant (Fig. 2c, d). This will be discussed further in the following section.

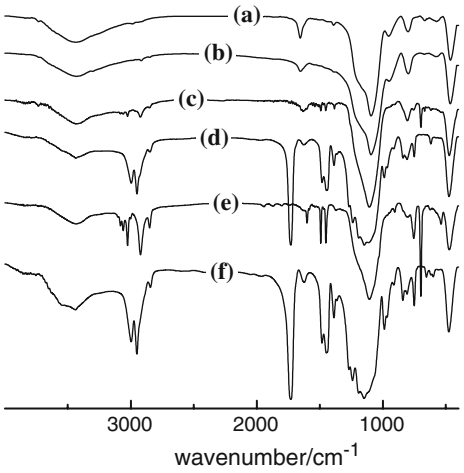

Fig. 2 IR spectra of (*a*) fumed silica, (*b*) aminated fumed silica, (*c*) fumed silica/PS (CTAB was used as the surfactant), (*d*) fumed silica/PMMA (CTAB), (*e*) fumed silica/PS (SDS), and (*f*) fumed silica/PMMA (SDS)

TGA analysis

The TGA curves in Fig. 3 a1, b1 indicate that the weight loss values of the polymer-grafted fumed silica are much larger than those of pristine and aminated fumed silica, no matter what kind of monomer and surfactant being used. This is in good agreement with the result of IR, which provides the evidence for the grafting of PMMA and PS onto fumed silica. The dTGA curves were shown in Fig. 3 a2 and b2. The weight loss rates of the fumed silica/PS and fumed silica/PMMA hybrid materials reach their maxima at 430 and 486 °C, respectively, and then decrease rapidly. The polymers and/or organic compounds on the surface of silica are almost completely removed at about 550 °C. The weight loss at temperatures above 550 °C can be attributed to the dehydration of the silanols in silica [41]. For pure PMMA and PS, the residual weights at 550 °C are 1.1 and 0 wt%, respectively. Therefore, the amount of PMMA and PS grafted on the fumed silica is determined based on the

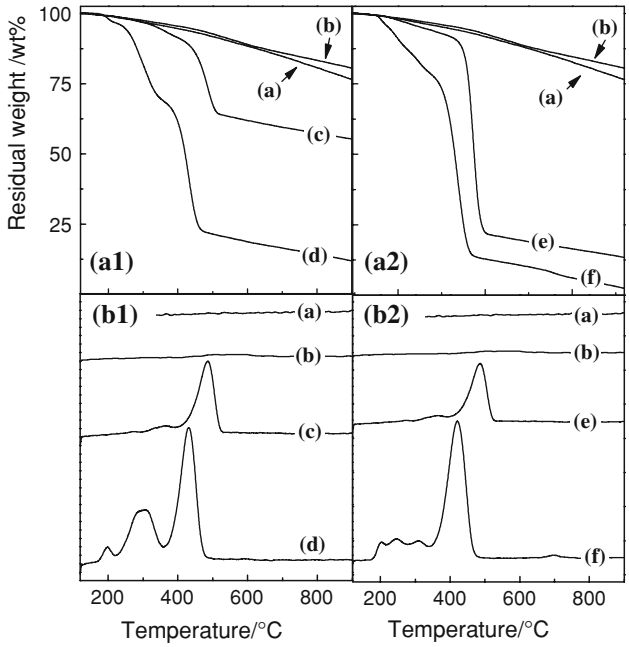

Fig. 3 TGA curves (**a1** and **b1**) and corresponding dTGA curves (**a2** and **b2**) of (*a*) pristine fumed silica, (*b*) aminated fumed silica, (*c*) fumed silica/PS (CTAB was used as the surfactant), (*d*) fumed silica/PMMA (CTAB), (*e*) fumed silica/PS (SDS), and (*f*) fumed silica/PMMA (SDS)

values of weight loss at 550 °C. The dTGA curves are almost the same for the two different surfactants, indicating that the type of surfactant has little influence on the thermogravimetric behavior of the polymers.

The grafting ratio W_g and monomer-to-polymer conversion of PMMA and PS grafted onto silica surfaces are quantitatively determined by the TGA curves according to Eqs. 1 and 2, respectively, as shown in Fig. 4. It is found that both the type of monomer and surfactant greatly affect the grafting ratio and polymerization conversion. For both CTAB and SDS, PMMA has higher grafting ratio and polymerization conversion than PS does. A possible explanation on this is the difference in the solubility of their monomers in water. For example, at 25 °C the solubility of MMA in water is about 1.5 wt% [42], which is about 50 times higher than that of styrene (about 0.03 wt% [43]). Because the redox initiation reaction occurs in the aqueous solution, the initiation of MMA should be easier than that of styrene. On the other hand, for both PMMA and PS, when SDS was used as the surfactant, the grafting ratio and polymerization conversion are much higher than those when CTAB was used as the surfactant. This is related to the difference in the electrostatic interaction between Ce(IV) and the two different surfactants during the emulsion graft polymerization. Sinha et al. [44] investigated the influence of cationic and anionic surfactants on the polymerization of acrylamide initiated by the Ce(IV)/cyclohexanone redox pair. It was found that CTAB decreased the polymerization kinetics, while SDS fastened the polymerization, decreased the overall activation energy

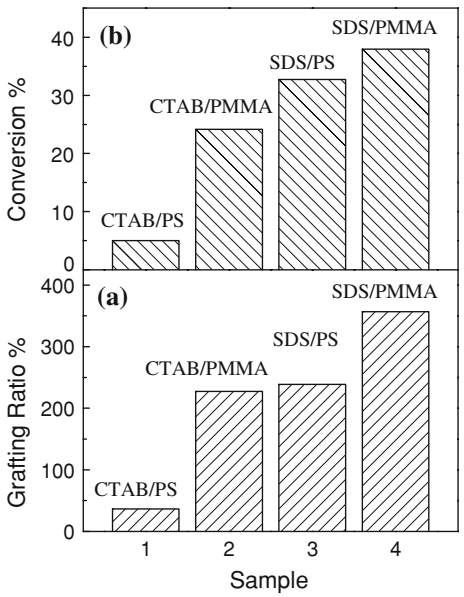

Fig. 4 Grafting ratios (**a**) and monomer-to-polymer conversions (**b**) for (1) fumed silica/PS (using CTAB as the surfactant), (2) fumed silica/PMMA (CTAB), (3) fumed silica/PS (SDS), and (4) fumed silica/PMMA (SDS)

and increased the molecular weight of the resultant polymer. It was proposed that the electrostatic interaction between Ce(IV) and SDS increased the concentration of Ce(IV) in the Stern layer of the SDS micelles and facilitated the initiation of polymerization, so that the polymerization and the percentage of monomer-to-polymer conversion were enhanced. For CTAB, the electrostatic repulsion between Ce(IV) and the cationic micelles leads to a restriction of the approach of Ce(IV) toward micellar-solubilized reductant and hindered the formation of free radicals. Differently, in this study, the reductant (i.e., aminated fumed silica) is water soluble, but the monomers are hydrophobic and solubilized in the surfactant micelles. Therefore, a reasonable explanation for the lower grafting ratio and monomer-to-polymer conversion when CTAB is used as the surfactant is that the repulsion interaction restricted the approach of Ce(IV) and the aminated fumed silica nanoparticles toward the micellar-solubilized monomers, so that the graft polymerizations were hindered to some extend.

Morphology and particle size

The TEM image in Fig. 5a shows that the pristine fumed silica nanoparticles have a diameter of about 10–12 nm. Because of the agglomeration of the fumed silica nanoparticles, branched networks morphology is observed in the TEM image, indicating that there exist strong attractive interparticle interactions among the fumed silica nanoparticles. In Fig. 5b, aggregation morphology of the aminated fumed silica is also observed. A possible explanation is that during the amination process, the pristine fumed silica nanoparticles themselves are not isolated but form aggregates due to van der Waals interparticle attraction, so that the aggregation is kept somehow during the followed preparation of the aminated particles. Similar agglomeration of nanoparticles during the functionalization process was also observed by some other authors [3, 45]. But fortunately, for the aminated fumed silica, most of the aggregated particles have sizes below 100 nm, which make it possible to prepare sub-100 nm polymer-grafted hybrid nanoparticles by graft polymerization as will be described later.

To observe the effect of surfactant on the stability of the graft polymerization, control experiments have been conducted, in which no surfactants were used. It was observed that a large amount of sediments appeared at the late stage of polymerization, because the silica nanoparticles turned from hydrophilic to hydrophobic after PMMA or PS was grafted onto their surfaces. On the contrary, both CTAB and SDS can effectively prevent macroscopic aggregation and the formation of precipitations during the emulsion graft polymerization.

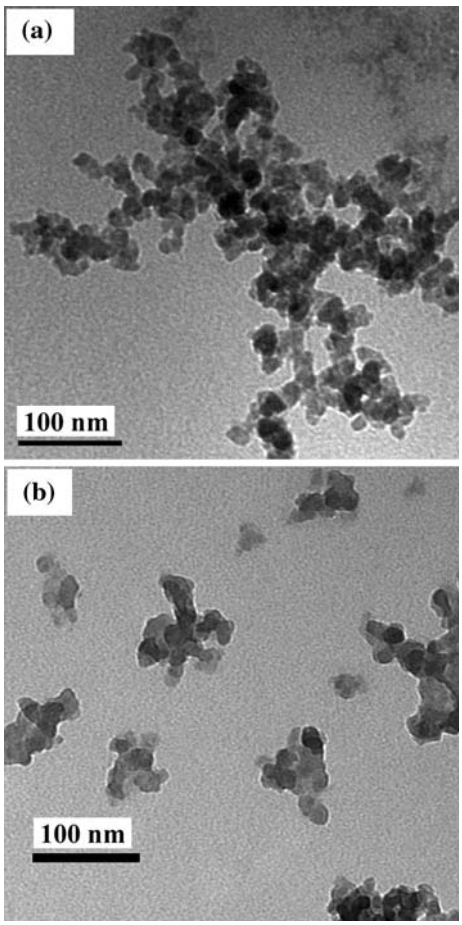

Fig. 5 TEM image of **a** pristine fumed silica and **b** aminated fumed silica

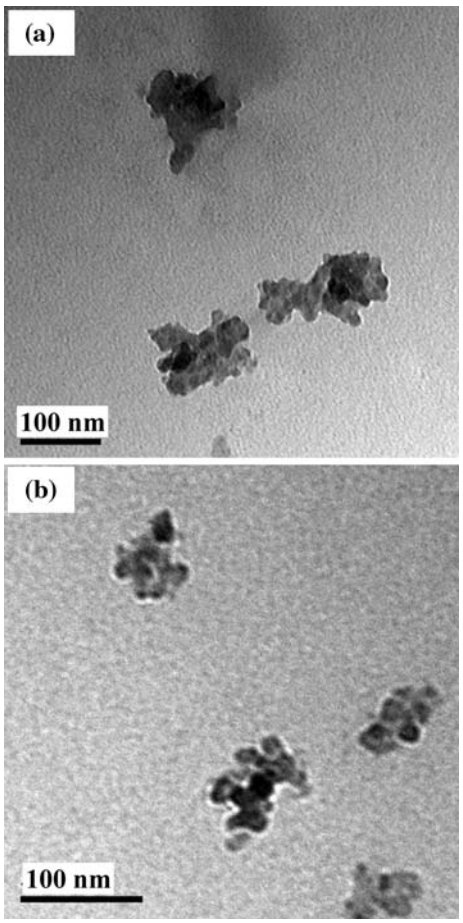

Fig. 6 TEM images of **a** fumed silica/PMMA and **b** fumed silica/PS hybrid nanoparticles with CTAB as the surfactant

Furthermore, it was found that CTAB and SDS have different effect on the morphology and size of the polymer-grafted particles. When CTAB was used as the surfactant, both the fumed silica/PMMA and fumed silica/PS particles are hybrid particles with particle sizes below 100 nm and a nonspherical and amorphous morphology, in which several fumed silica nanoparticles form the core with PMMA or PS existing around the silica nanoparticles (Fig. 6a, b). No single PMMA or PS encapsulated fumed silica nanoparticles with a well-defined core–shell structure are observable in TEM, but fortunately, the particles are sub-100 nm sized, i.e., nanoparticles. The particle sizes of the aminated and polymer-grafted silica particles were further determined by DLS, which are in satisfactory agreement with the results of TEM. As shown in Fig. 7a, most of the aminated fumed silica (about 97%) have diameters from 37 to 50 nm. Whereas, the particle size of about 98.5% of the fumed silica/PMMA hybrid nanoparticles is in the range of 75–90 nm, which is somewhat larger than that of the aminated silica. About 1.5% of the particles are aggregates having an average particle size of about 265 nm (Fig. 7b). Similarly, the particle size of about 97.5% of the fumed silica/PS hybrid nanoparticles is about 57–85 nm, which is also somewhat larger than that of aminated silica. A small quantity (about 2.5%) of the hybrid particles has an average particle size of 265 nm (Fig. 7c). Therefore, both TEM and DLS results indicated sub-100 nm sized nanoparticles of fumed silica/PMMA and fumed silica/PS hybrids can be successfully obtained when CTAB was used as the surfactant.

In contrast to CTAB, when the anionic surfactant SDS was used in the graft polymerization, the size and morphology of the PMMA and PS-grafted fumed silica are totally different. The TEM images in Fig. 8 showed that the PMMA-grafted fumed silica coagulated into clusters larger than 100 nm with an irregular morphology, and the PS-grafted fumed silica has a network morphology (as indicated by the arrows in Fig. 8b). A possible explanation on the mechanism of the morphology is the electrostatic attractions between the cationic Ce(IV) ions, aminated silica nanoparticles, and the anionic SDS molecules, which bring about the interparticle coupling of the polymer-

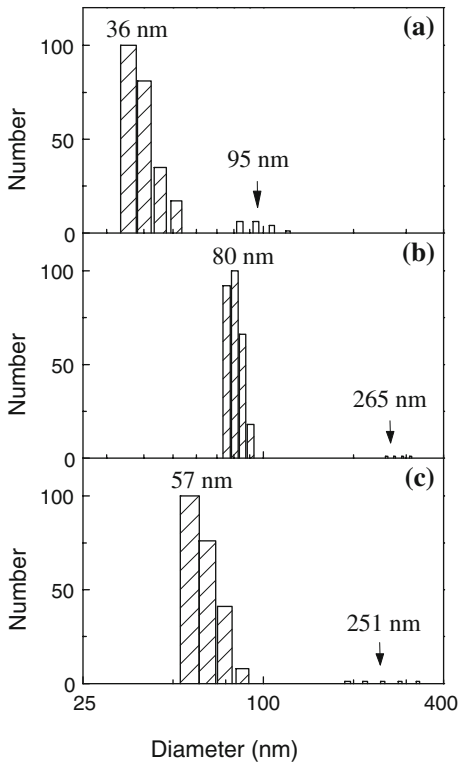

Fig. 7 Particle size distribution measured by DLS of **a** aminated fumed silica, **b** fumed silica/PMMA, and **c** fumed silica/PS hybrid nanoparticles with CTAB as the surfactant

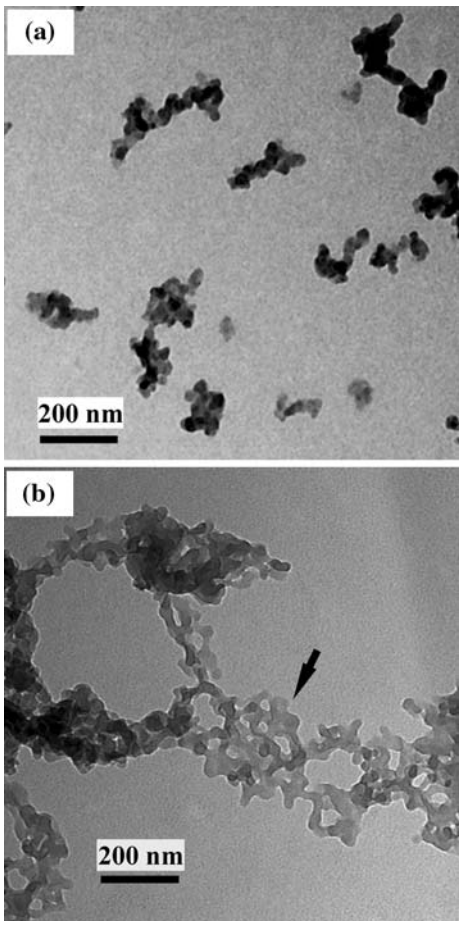

Fig. 8 TEM images of **a** fumed silica/PMMA and **b** fumed silica/PS hybrid particles with SDS as the surfactant

grafted fumed silica during the emulsion polymerization. Previous study [46] has demonstrated that Ce(III) and SDS form aggregates in aqueous solution, resulting in apparent changes in the conductivity and light scattering intensity of the solution. Therefore, it is reasonable to believe that similar aggregates form in the mixture of Ce(IV) and SDS in this study. Polymerization of MMA and styrene further facilitated the formation and growth of the aggregates. Therefore, sub-100 nm hybrid particles were not obtained when SDS was used as the surfactant.

The disadvantage of the present Ce(IV)/amine redox system is that it does not allow the fabrication of well isolated and core–shell structured nanoparticles with a single core and a uniform shell. This results from the agglomerated structure of the aminated fumed silica and further agglomeration during emulsion polymerization. However, at least when CTAB was used as the surfactant, fumed silica/PMMA and fumed silica/PS hybrid nanoparticles with particle sizes below 100 nm were successfully obtained and the grafting ratio and monomer-to-polymer conversion are satisfactory. Such hybrid nanoparticles can be potentially used as additives for coatings, adhesives, and resins to improve the mechanical properties, heat resistance, and abrasion resistance of the polymer matrix. At the same time, it is able to allow a facile and mild graft polymerization at low temperatures in aqueous solutions, and is versatile for many monomers.

Summary

In this article, graft polymerization of hydrophobic polymers onto fumed silica nanoparticles was conducted in emulsions with CTAB and SDS as the surfactants. The polymerization was initiated by the redox reaction between Ce(IV) and the aminated fumed silica. Surfactants stabilized the emulsion system and prevented the occurrence of precipitation during polymerization. IR and TGA results indicated that both PMMA and PS were successfully grafted onto the fumed silica. It was found that both the type of monomer and surfactant have important influences on the emulsion graft polymerization. The grafting ratio and monomer-to-polymer conversion of PMMA are higher than those of PS, possibly due to the higher solubility of MMA in water. When SDS was used as the surfactant, both the grafting ratio and monomer-to-polymer conversion are

higher, but the particles coagulated into large clusters with irregular morphology or even networks, due to the electrostatic interactions between SDS and ceric ions and/or the aminated fumed silica nanoparticles. But fortunately, when CTAB was used as the surfactant, the resultant particles were sub-100 nm nonspherical nanoaggregates comprising several fumed silica nanoparticles as the core and polymers existing around the nanoparticles. The particles sizes of the fumed silica/PMMA and fumed silica/PS hybrid nanoparticles are 75–90 and 57–85 nm, respectively.

Acknowledgments We greatly appreciate financial support from the National Natural Science Foundation of China (NNSFC No. 20574060 and No. 50773066).

References

1. Pyun J, Jia SJ, Kowalewski T, Patterson GD, Matyjaszewski K (2003) Macromolecules 36:5094
2. Park JH, Woo S, Kim JH, Kim R, Kim J, Lee SS (2008) Mater Lett 62:3916
3. Mori H, Seng DC, Zhang M, Muller AHE (2002) Langmuir 18:3682
4. Jang I, Sung J, Choi H, Chin I (2005) J Mater Sci 40:3021. doi: 10.1007/s10853-005-2381-1
5. Xu H, Cui LL, Tong NH, Gu HC (2006) J Am Chem Soc 128:15582
6. Zhang JG, Coombs N, Kumacheva E (2002) J Am Chem Soc 124:14512
7. Gittins DI, Caruso F (2001) J Phys Chem B 105:6846
8. Guyot A, Landfester K, Schork FJ, Wang CP (2007) Prog Polym Sci 32:1439
9. Auroy P, Auvray L, Léger L (1992) J Colloid Interface Sci 150:187
10. Ebata K, Furukawa K, Matsumoto N (1998) J Am Chem Soc 120:7367
11. Zhang ZK, Berns AE, Willbold S, Buitenhuis J (2007) J Colloid Interface Sci 310:446
12. Zhang K, Chen HT, Chen X, Chen ZM, Cui ZC, Yang B (2003) Macromol Mater Eng 288:380
13. Gu SC, Onishi J, Mine EC, Kobayashi Y, Konno M (2004) J Colloid Interface Sci 279:284
14. Zhou J, Zhang SW, Qiao XG, Li XQ, Wu LM (2006) J Polym Sci A Polym Chem 44:3202
15. Zhang SW, Zhou SX, Weng YM, Wu LM (2005) Langmuir 21:2124
16. Prucker O, Rühe J (1998) Macromolecules 31:592
17. Bachmann S, Wang HY, Albert K, Partch R (2007) J Colloid Interface Sci 309:169
18. Kim S, Kim E, Kim S, Kim W (2005) J Colloid Interface Sci 292:93
19. Chen XY, Randall DP, Perruchot C, Watts JF, Patten TE, von Werne T, Armes SP (2003) J Colloid Interface Sci 257:56
20. von Werne T, Patten TE (1999) J Am Chem Soc 121:7409
21. Perruchot C, Khan MA, Kamitisi A, Armes SP, von Werne T, Patten TE (2001) Langmuir 17:4479
22. Wang YP, Pei XW, He ZY, Yuan K (2005) Eur Polym J 41:1326
23. Barner L, Zwaneveld N, Perera S, Pham Y, Davis TP (2002) J Polym Sci A 40:4180
24. Hong CY, Li X, Pan CY (2007) Eur Polym J 43:4114
25. Parvole J, Montfort JP, Billon L (2004) Macromol Chem Phys 25:1369
26. Bartholome C, Beyou E, Bourgeat-Lami E, Chaumont P, Zydowicz N (2003) Macromolecules 36:7946
27. Parvole J, Billon L, Montfort JP (2002) Polym Int 51:1111
28. Kasseh A, Ait-Kadi A, Riedl B, Pierson JF (2003) Polymer 44:1367
29. Blomberg S, Ostberg S, Harth E, Bosman AW, van Horn B, Hawker CJ (2002) J Polym Sci A 40:1309
30. Bamford CH, Al-Lamee KG (1994) Macromol Rapid Commun 15:379
31. Shuckla SR, Athalye AR (1994) J Appl Polym Sci 54:279
32. Fanta GF, Burr RC, Doane WM (1984) J Appl Polym Sci 29:4449
33. Mino G, Kaizerman S (1958) J Polym Sci 31:242
34. Odian G, Kho JHT (1970) J Macromol Sci Chem A 4:317
35. Gupta KC, Sahoo S (2000) J Appl Polym Sci 76:906
36. Ranby B, Zuchowska D (1987) Polym J 19:623
37. Wang YP, Yuan K, Li QL, Wang LP, Gu SJ, Pei XW (2005) Mater Lett 59:1736
38. Wang H, Peng M, Zheng J, Li P (2008) J Colloid Interface Sci 326:151
39. Sui KY, Gu LX (2003) J Appl Polym Sci 89:1753
40. Sarac AS (1999) Prog Polym Sci 24:1149
41. Iler RK (1979) The chemistry of silica: solubility, polymerization, colloid and surface properties and biochemistry of silica. Wiley, New York
42. Ming WH, Jones FN, Fu SK (1998) Polym Bull 40:749
43. Lane WH (1946) Ind Eng Chem Anal Ed 18:295
44. Patra M, Sinha BK (1998) Macromol Chem Phys 199:311
45. Bombalski L, Min K, Dong HC, Tang CB, Matyjaszewski K (2007) Macromolecules 40:7429
46. Valente AJM, Burrows HD, Cruz SMA, Pereira RFP, Ribeiro ACF, Lobo VMM (2008) J Colloid Interface Sci 323:141